Rev. Roum. Sci. Techn.– Électrotechn. et Énerg.
Vol.70, 4, pp. 525–530, Bucarest, 2025

MINIATURIZED AND CIRCULAR POLARIZED METAMATERIAL-INSPIRED ANTENNA FOR WIRELESS COMMUNICATION

PARAMANAND SHARMA[1], SAPTARSHI GUPTA[1], VIBHAV KUMAR SACHAN[2], DIVYA SAXENA[3]

Keywords: Circular polarized antenna; Triple-band antenna; Metamaterial-inspired antenna; 5G applications; Wireless local area network (WLAN) applications.

In this paper, a miniaturized triple-band antenna is designed for wireless communication applications. The two inverted C-shaped strips are used to enhance the electric length, which improves the impedance bandwidth. The unit cell analysis of the inverted C-shaped strips indicates that the three bands are directly responsible for the negative permeability. The triangular-shaped parasitic stub is used in the ground to perturb the surface waves, which affects the CP behavior of the antenna at higher operating bands. The antenna bandwidths are obtained as follows: 2.37 GHz (2.337–2.405 GHz), 3.34 GHz (3.06–3.84 GHz), and 5.21 GHz (5.08–5.38 GHz), where the axial ratio is attained from 5 GHz to 5.35 GHz. The miniaturized size and triple-band antenna are well-suited for portable applications that require a compact design.

1. INTRODUCTION

In recent times, the demand for multi-band microstrip antennas is increasing due to the increasing use of wireless communications. A useful solution to meet the demand for multi-band service is to build a single broadband antenna that can cover all applications/bands. Multiband antennas are an important development in recent multifunctional wireless communication systems because they can resonate at multiple frequencies, eliminating the need for multiple antennas in a single unit [1–5]. As the utility of portable devices increases, the miniaturization of antennas is becoming increasingly compact, meeting the requirements of a compact size, good gain, acceptable radiation characteristics, and high impedance matching (IM).

Over the years, researchers have used multiband and miniaturized antenna technology such as SRR/CSRR [3], MTM [4, 14], Open-ended stub [2, 5–8], parasitic strip [5], bisection method [7], slots/stub [1, 10–12], defected ground [1, 9, 11–13]. In [1], stubs and defective ground are used to improve the impedance matching of the antenna for dual-band response. In [2], slots and stubs on the patch are accomplished to obtain the mutual impedance for multiband operation. The slots in the patch perturb the electric length and reduce the frequency band towards a lower frequency. In [3], MTM structure-inspired ground is loaded on the slot antenna, which improves the gain of the antenna and is responsible for multi-bands. In [4], SRR is achieved in the radiator, which exhibits MTM behavior and is responsible for the triple bands. In [5], an Open-ended stub and parasitic strip are used in the multiband antenna for impedance matching. In [6], open-ended stubs are implemented to optimize the circular patch antenna and to accomplish miniaturization and dual bands. In [7], the bisection method is used to miniaturize the antenna, where the slot is used in the ground for impedance matching. In [8], the open-ended slots are inserted on the radiator to improve the IM of the partial ground antenna. In [9], defective ground and slots in the radiator are used to design the compact antenna for C and S bands. In [10], CPW fed with ground is used, where multiple strips are used to obtain multiple bands. In [11], the slot and defective ground multiband antenna are designed where defected ground, slot in the patch, and modified feed line are used to obtain the multiband operation. In [12], multiple slots with shorting pins are introduced on the microstrip patch to achieve the dual-band response with high gain. In [13], defected ground is used to improve the impedance matching of a microstrip-fed TL radiator, where the multiple slots in the ground are responsible for triple-band operation. In [15], multiple SRR radiators with a modified partial ground are used to achieve a dual-band response. In [16], defective ground and slots on the patch are utilized to enhance the impedance matching of the antenna, with the feed position also optimized to achieve a dual-band response. In [17], a defected ground is used to design the UWB antenna, and a parasitic notch is used to eliminate the undesired band so that the antenna can also work as a dual-band antenna. As per the study of the recently published work, a triple band antenna is designed with circularly polarized behavior for wireless communication and can be the perfect choice for wearable applications, as miniaturized in size. The novelty and technical advancement of the presented work are discussed below.

a) The antenna is implemented on the FR-4 material, which is a popular material used in wireless communication devices at a low cost.
b) The two inverted novel C-shaped strips on the microstrip feed are used to improve the bandwidth of the antenna. The unit cell of the C-shaped strip analysis represented the negative permeability at 2.4/4.5/5.5 GHz and helped to achieve the triple operating bands, where the operating frequencies of the antenna are shifted due to optimization.
c) The miniaturized size of the antenna is $0.158\ \lambda \times 0.197\ \lambda$; therefore, it can be used in a portable application where a small antenna size is required.
d) The triangular parasitic strip in the ground is used to perturb the surface current and change the LP to CP behavior of the antenna in the higher operating band.

The antenna operates the LP behavior in the first and second operating bands, whereas the CP operates in the third operating band; therefore, the triple operating band antenna covers both LP and CP polarization.

2. DESIGN AND ANALYSIS OF CP ANTENNA

In this paper, an MTM-inspired triple-band antenna is

[1] Department of Electronics and Communication Engineering, SRM Institute of Science and Technology, Delhi-NCR Campus, Modinagar, Ghaziabad, Uttar Pradesh, 201204, India.
[2] Department of Electronics and Communication Engineering, KIET Group of Institutions, Delhi-NCR, Ghaziabad, Uttar Pradesh, 201206, India.
[3] Department of Applied Science & Humanities, ABES Engineering College, Ghaziabad, Uttar Pradesh, 201009, India.
E-mails: ps8277@srmist.edu.in, saptarsg@srmist.edu.in, vibhav.sachan@kiet.edu, divya.saxena@abes.ac.in

DOI: 10.59277/RRST-EE.2025.70.4.16

implemented with CP behavior, where the antenna size is miniaturized. The prototype, with its dimensions and hardware, is demonstrated in Fig. 1(a). The design steps of the antenna are described in Fig. 1(b), which is divided into five parts, and its S_{11} parameters are illustrated in Fig. 1(c). The single-element monopole antenna is designed using a popular material (FR-4), with a substrate thickness of 1.6 mm. In the first steps, the simple monopole antenna is used with the partially defected ground, where the microstrip-fed is accomplished to achieve the IM of 50 Ω.

The microstrip feed width and length are set to 3 mm and 1.5 mm, respectively, to achieve a 10 dB impedance bandwidth.

The operating bandwidth varies from 5.95 GHz to 6.5 GHz. In the second step, the inverted C-shaped strip is accomplished on the microstrip feed line, which increases the electric length. The IBW of the antenna is found at 2.45 GHz and from 4.8 GHz to 5.8 GHz. In the third step, another inverted C-shaped strip is formed on the microstrip line, as depicted in Fig. 1(b), labeled as step 3. This strip also increases the length of the antenna and improves the bandwidth, extending from 3.1 GHz to 3.6 GHz and from 5.9 GHz to 6.3 GHz. In the fourth step, both inverted C-shaped strips introduced in steps 2 and 3 are demonstrated, which helps achieve a triple operating band. Additionally, the size of the antenna is miniaturized compared to the conventional antenna discussed in step 1.

The IBW is obtained in 2.35 GHz, 3 GHz to 3.6 GHz, and 5.1 GHz to 5.75 GHz. In this fifth step, a novel triangular-shaped metallic parasitic element is placed on the ground to influence the current and enhance the antenna performance. The parasitic element perturbs the surface current, allowing the antenna to achieve LP to CP on the higher operating bands. The axial ratio (3 dB) of the antenna is found to be between 5 GHz and 5.35 GHz, as demonstrated in Fig. 1(d).

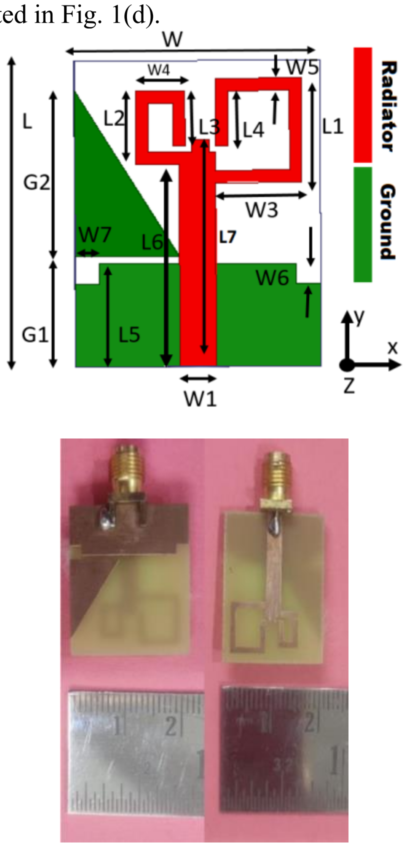

(a)

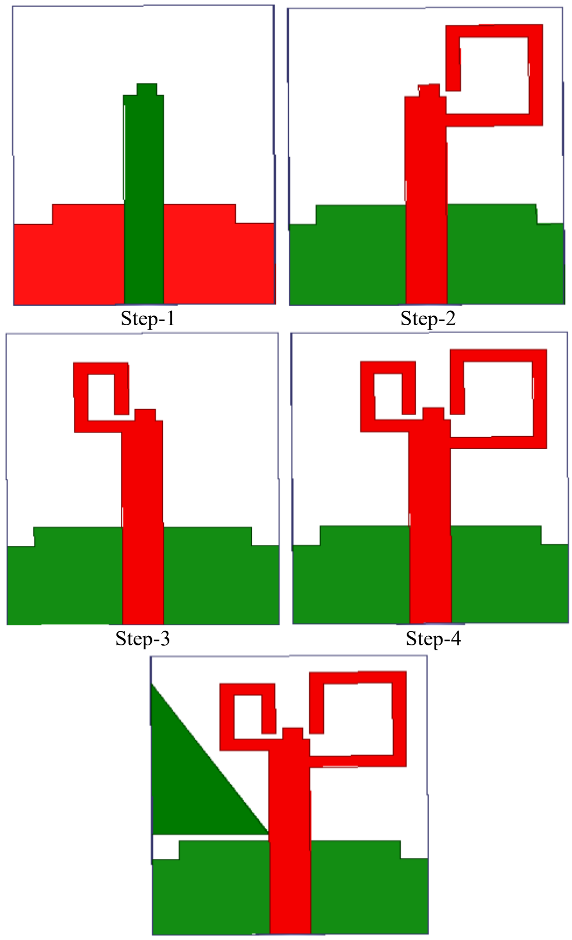

(b)

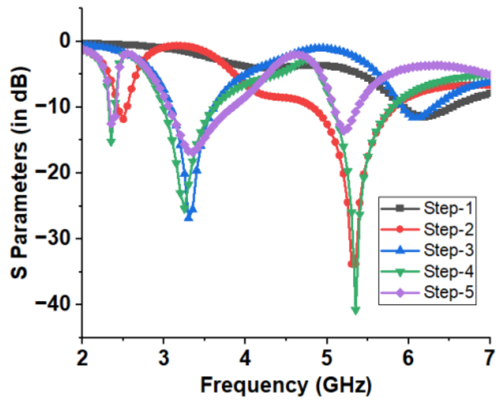

(c)

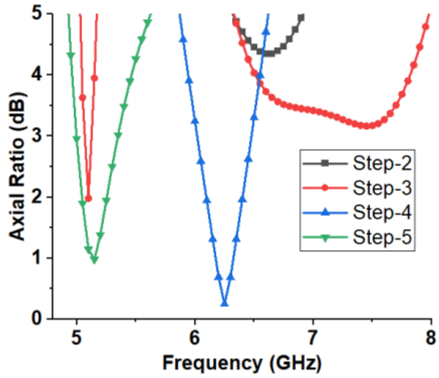

(d)

Fig. 1 – Proposed Triple band antenna (a) Designed prototype (Parameters in mm – L=25, W=20, G1=9, G2=13.5, L1=8.5, L3=4.5, L4=4.5, L2=6, L5=8.375, L6=16.5, W7=2, W5=1, W1=3, W6=2.25, W4=4, W3=7, L7=18.5) (b) antenna steps (c) s-parameters (d) Axial ratio.

3. ANALYSIS OF CP BEHAVIOUR OF PROPOSED ANTENNA

The circular polarization of the antenna is analyzed at the higher frequency band. The triangular parasitic stub is used to perturb the current behavior, which influences the antenna from an LP antenna to a CP antenna. The 3dB axial ratio of the antenna covering almost a full third of the operating band varies from 5 GHz to 5.35 GHz, where the IBW of the antenna is 5.08 GHz to 5.38 GHz. The surface current movement at 5.2 GHz is illustrated in Fig. 2(a-d), where the current movements are depicted at 0°, 90°, 180°, and 270° phases. The variation of the surface current at different angles reveals that the surface current in the ground is perturbed in an anticlockwise direction; therefore, the antenna exhibits RHCP behavior. The combination of an LP antenna at the lower operating band and a CP in the higher operating band can be a good practical application in wireless communication.

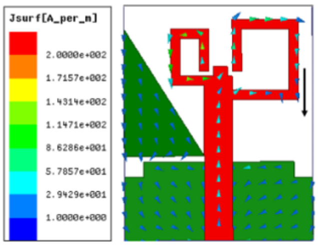

(a)

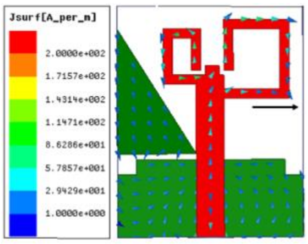

(b)

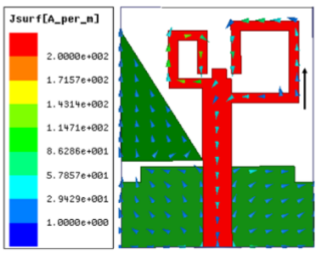

(c)

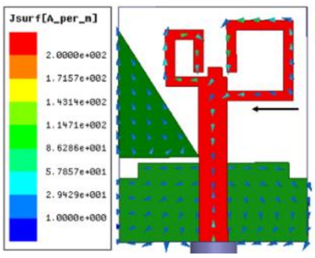

(d)

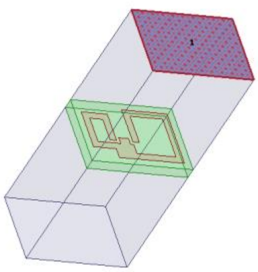

(e)

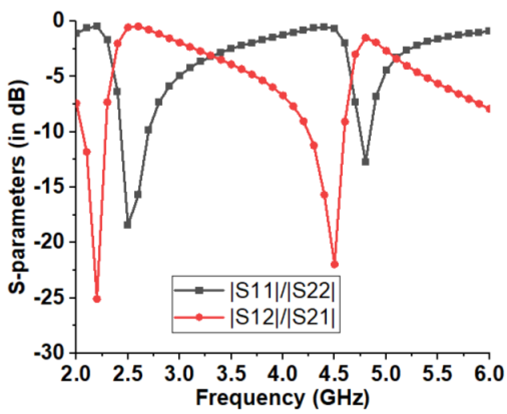

(f)

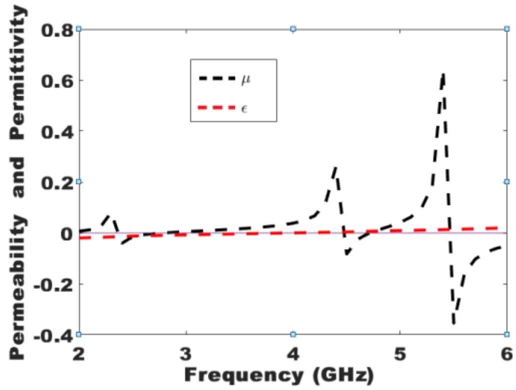

(g)

Fig. 2 – CP Analysis of the triple band antenna: (a) 0º; (b) 90º; (c) 270º; (d) 360º; (e) Unit cell (f); S-parameters of the unit cell; (g) Permeability and permittivity of the unit cell.

The metamaterial behaviour of the antenna is studied with the unit cell of the radiator as demonstrated in Fig. 2(e), where the wave port with PEC and PMC boundary conditions is used to determine the S-parameters as demonstrated in Fig. 2(f). The metamaterial characteristics are demonstrated in Fig. 2(g). The Nicolson Ross Weir [14] equations with wave vector (Ko) and the thickness (d) are utilized from:

$$V_1 = S_{11} + S_{21}, \tag{1}$$

$$V_2 = S_{21} - S_{11}, \tag{2}$$

$$\mu_r \sim \frac{(1-V_2)}{(1+V_2)} \frac{2}{jk_0 d}, \tag{3}$$

$$\varepsilon_r \sim \frac{(1-V_1)}{(1+V_1)} \frac{2}{jk_0 d} \tag{4}$$

The S-parameters of the unit cell are depicted as the dual-band response of the passband and the stopband. The MTM characteristics of the unit cell are represented in Fig. 2(g), which shows the negative permeability at 2.4/4.5/5.5 GHz, where the permittivity is near zero and positive after 4 GHz, and negative before 3 GHz. The Permeability of the unit cell indicated that the negative permeability of the unit cell is responsible for the triple a-band antenna, where the antenna resonant frequencies are 2.37 GHz, 3.34 GHz, and 5.21 GHz, and validates the MTM-inspired behavior.

4. SIMULATED AND EXPERIMENTAL RESULTS ANALYSIS

The triple-band antenna is designed on the HFSS-13 software, and the MTM antenna is validated using Anritsu MS2025B VNA. The s-parameters ($|S_{11}|$) of the triple band antenna are illustrated in Fig. 3(a), where 10 dB IBW varies from 2.337–2.405 GHz, 3.06 –3.84 GHz, and 5.08 – 5.38 GHz, and are close to the measured results. The circular analysis from a 3 dB axial ratio of the triple band antenna varies from 5 GHz to 5.35 GHz and is close to the measured results as demonstrated in Fig. 3(b).

The simulated and measured values of the gain are 0.9 dB and 0.5 dB at 2.35 GHz, 2.3 dB and 1.7 dB at 3.3 GHz, and 2.5 dB and 3 dB at 5.2 GHz, as represented in Fig. 3(c), which shows good agreement with measured results. The simulated efficiency is 76 %at 2.35 GHz, 2.3 dB, and 95% at 3.3 GHz, and 84 % at 5.2 GHz, as demonstrated in Fig. 3(d), which shows the higher efficiency in all the bands. The measuring set-up in anechoic chambers is exemplified in Fig. 3(e). The radiation pattern in the normalized form is represented in Fig. 3(f) and 3(g).

The linear pattern at 3.3 GHz is demonstrated in Fig. 3(f) at the xz and yz planes, where a more than 20 dB difference between the co-and cross-plane is achieved. The RHCP pattern of the antenna at 5.25 GHz is illustrated in Fig. 3(g), which shows the stable radiation patterns. The relative analysis of the MTM antenna in comparison to existing work is illustrated in Table 1. The proposed antenna size is miniaturized and operates in a triple band, exhibiting both linear and circular polarization behavior, which makes it applicable in antennas for wireless and wearable communications.

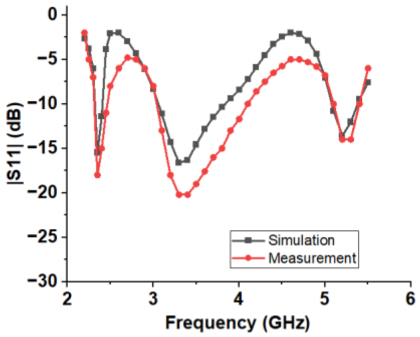

(a)

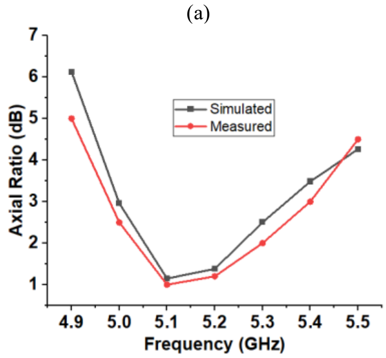

(b)

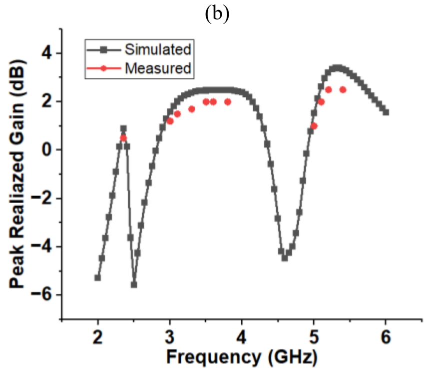

(c)

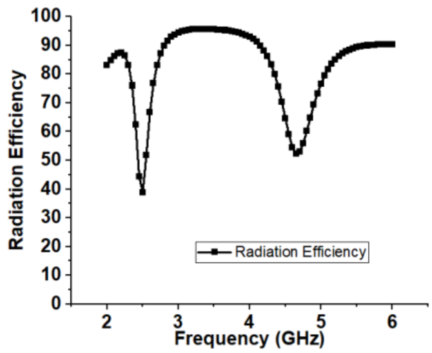

(d)

(e)

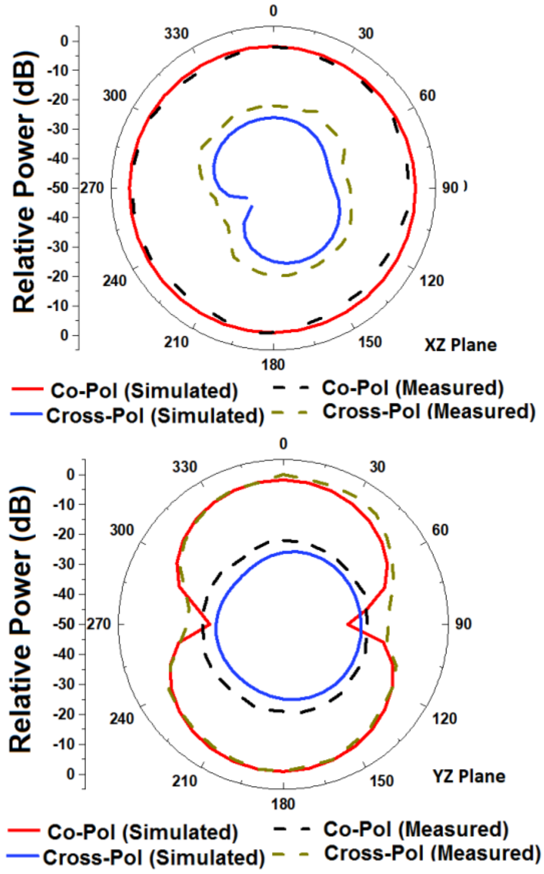

(f)

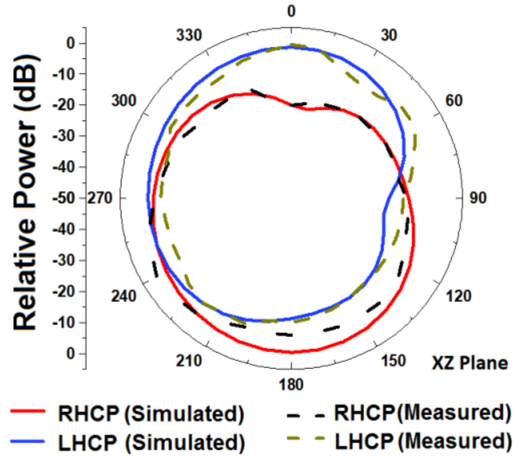

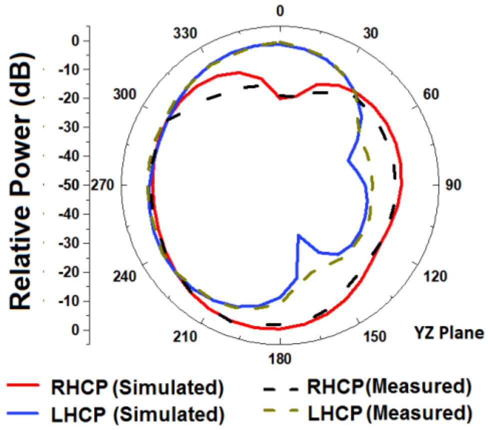

(g)

Fig. 3 – Antenna analysis: (a) S-parameters (dB); (b) Axial ratio (3-dB); (c); Gain (dB); (d) Radiation efficiency (%); (e) Measuring set-up; (f) Radiation pattern at 3.3 GHz, and (g) Radiation pattern at 5.25 GHz.

5. CONCLUSION

In this work, the size of the antenna is reduced with an MTM-inspired radiator, and linear polarization is achieved at 2.37/3.34 GHz, and circular polarization is achieved at 5.21 GHz. The metamaterial unit cell has been investigated, and it was found that the permeability of the radiator is responsible for triple bands. The triangular shape parasitic stub is loaded in the ground of the triple band antenna, which shifted the axial ratio towards the operating bands. The triple-band antenna operates from 2.337–2.405 GHz, 3.06–3.84 GHz, and 5.08–5.38 GHz, with CP performance from 5 GHz to 5.35 GHz. The antenna's overall size is compact and miniaturized, which makes the antenna applicable for portable applications.

CREDIT AUTHORSHIP CONTRIBUTION

Author_1: Paramanand Sharma worked on methodology, design concept, metamaterial analysis, simulations, measurements, and writing of the paper.
Author_2: Saptarshi Gupta has supervised the work and simulation as well as reviewed the manuscript.
Author_3: Vibhav Sachan has supervised the work and measurement as well as reviewed the manuscript.
Author 4: Divya Saxena contributed to the design concept and metamaterial analysis of the manuscript.

Received on 26 September 2024

Table 1
Relative investigation with compact and multiband antenna

[Ref No.] (publication year)	Antenna Size (mm^2)	Resonant Frequency (GHz)	No. of band	Technology used	CP
Proposed	20 × 25	2.37, 3.34, 5.21	3	MTM structure with parasitic stub	Yes
[1] (2020)	33 × 17	2.5, 3-6.65	2	Defected ground and stub	No
[2] (2023)	56.4 ×44.3	3.34, 4.61, 6.01 and 8.02	4	Slot and stubs	No
[3] (2023)	60 ×60	3.02, 4.14, 4.96, 5.44 and 5.8	5	CSRR/MTM	No
[4] (2022)	20 × 30	2.34, 3.32 and 6.5	3	MTM	No
[5] (2019)	75 × 120	0.96 and 1.8	2	Open ended stub and parasitic strip	No
[6] (2020)	32×32	5.19, 5.87	2	Open-ended stub	No
[7] (2020)	15 × 15	6.2	1	Circle slot in the ground	No
[8] (2019)	15 × 15	4.2, 9.9	2	Modified open-ended slot	No
[9] (2021)	26.11 × 24.81	3.56 and 4.07	2	Slot in the patch, stub in the ground	No
[10] (2022)	26 ×13	2.4, 4.5, 5.5, 6.5, and 7.8	5	Multiple stubs	No
[11] (2023)	33× 24	4.36,8.25,10.01,12.00 and 15.89	5	Slot and Defected ground	No
[12] (2024)	55.3× 47	5.82 and 6.48	2	Shorting pins and stubs	No
[13] (2023)	20 × 21	3, 6.1, 8.2	3	Defected ground	No
[14] (2023)	25 × 22	2.4, 3.5, and 5.8	3	MTM	No
[15] (2023)	15 × 35	2.3–2.5, 3.5 up to 9	2	SRR and defected ground	Yes
[16] (2023)	9.2 × 9.2	2.4 and 5.8	2	Slots and Defected ground	Yes

REFERENCES

1. M. Karthikeyan et al., *Compact multiband CPW-fed monopole antenna with square ring and T-shaped strips*, Microwave and Optical Technology Letters, **62**, pp. 926–932 (2020).
2. B.G. Hakanoglu et al., *Crown-shaped edge multiband antenna design for 5G and X-Band applications*, Wireless Networks, pp. 1–16 (2023).
3. P. Jha, A. Kumar, and N. Sharma, *A Metamaterial-inspired split ring resonator accomplished multiband antenna for 5G and other wireless applications*, Rev. Roum. Sci. Techn. – Électrotechn. et Énerg., **68**, *2*, pp. 127–131 (2023).
4. P. Jha, A. Kumar, A. De, and R.K. Jain, *CPW-fed metamaterial inspired compact multiband antenna for LTE/5G/WLAN communication*, Frequenz, **76**, *7–8*, pp. 401–407 (2022).
5. J.Y. Deng, S.Y. Liu, D.Q. Sun, L.X. Guo, and S.B. Xue, *Multiband antenna for mobile terminals*, International Journal of RF and Microwave Computer Aided Engineering, **29**, *11*, e21925 (2019).
6. M. Shaw, N. Mandal, and M. Gangopadhyay, *A low-profile miniaturized circular microstrip patch antenna for dual-band application*, Frequenz, **74**, *9–10*, pp. 333–349 (2020).
7. W. Yibo, W. Shuyue, and Z. Jinju, *Bandwidth enhanced miniaturized slot antenna on a thin microwave laminate*, AEU-International Journal of Electronics and Communications, **127**, 153475 (2020).
8. A. Peram, S.R. Reddy, and G. Prasad, *Miniaturized single-layer ultra-wideband (UWB) patch antenna using a partial ground plane*, Wireless Personal Communications, **106**, *3*, pp. 1275–1291 (2019).
9. B.A. Sheik, P.V. Sridevi, and P.V. Rama Raju, *A Compact Wideband Rectangular Microstrip Antenna to the S and C Bands Applications*, Wireless Personal Communications, **121**, *1*, pp. 597–619 (2021).
10. I. Ahmad et al., *Highly compact GCPW-fed multi-branch structure multi-band antenna for wireless applications*, International Journal of Antennas and Propagation (2022).
11. A.G. Mamatha and P.M. Hadalgi, *Compact spiral-shaped slot-loaded antenna for multiband application*, Microsystem Technologies, pp. 1–7 (2023).

12. L. Jin and R. Zhang, *A dual-band wideband high-gain slot-loaded microstrip patch antenna*, AEU-International Journal of Electronics and Communications, **155**, 193 (2024).
13. M.A. Gaber et al., *Characteristic modes of a slot antenna design based on defected ground structure for 5G applications*, Scientific Reports, **13**, *1*, 15327 (2023).
14. D. Saxena et al., *Metamaterial-inspired dual band MIMO antenna with open-ended slot and neutralized line for isolation enhancement*, 10th International Conference on Signal Processing and Integrated Networks (SPIN), IEEE (2023).
15. D.N. Elshaekh et al., *Printed circularly polarized split-ring resonator monopole antenna for energy harvesting*, Ain Shams Engineering Journal, **14**, *6*, 102182 (2023).
16. S. Mosavinejad et al., *A triple-band spiral-shaped antenna for high data rate fully passive implantable devices*, AEU-International Journal of Electronics and Communications, **159**, 154474 (2023).
17. P. Gupta, M. Bharti, and A. Kumar, *Compact two-port antenna with parasitic notch and defective ground for wireless communication*, Rev. Roum. Sci. Techn. – Électrotechn. et Énerg., **68**, *4*, pp. 401–406 (2023).